STARS

University of Central Florida
STARS

Honors Undergraduate Theses UCF Theses and Dissertations

2022

Impact of Proton and Neutron Irradiation on Carrier Transport Properties in GA2O3

Andrew C. Silverman
University of Central Florida

Part of the Physics Commons

Find similar works at: https://stars.library.ucf.edu/honorstheses
University of Central Florida Libraries http://library.ucf.edu

This Open Access is brought to you for free and open access by the UCF Theses and Dissertations at STARS. It has been accepted for inclusion in Honors Undergraduate Theses by an authorized administrator of STARS. For more information, please contact STARS@ucf.edu.

Recommended Citation

Silverman, Andrew C., "Impact of Proton and Neutron Irradiation on Carrier Transport Properties in GA2O3" (2022). *Honors Undergraduate Theses*. 1209.
https://stars.library.ucf.edu/honorstheses/1209

IMPACT OF PROTON AND NEUTRON IRRADIATION ON CARRIER TRANSPORT PROPERTIES IN GA_2O_3

by

ANDREW C. SILVERMAN

A thesis submitted in partial fulfilment of the requirements
for the Honors in the Major Program in Physics
in the College of Sciences
and in the Burnett Honors College
at the University of Central Florida

Spring Term
2022

Thesis Chair: Dr. Elena Flitsiyan

ABSTRACT

This project studies the properties of minority charge carriers in beta gallium oxide (β-Ga_2O_3). The behavior of minority carriers is of high importance as it greatly affects conduction and consequently device performance. Cathodoluminescence (CL) spectroscopy and EBIC (Electron Beam Induced Current) are the main experimental techniques used to study minority carrier behavior.

High energy radiation affects minority carrier properties through damage to the material and through the production of carrier traps that reduce the conductivity and mobility of the material. In this investigation, we study the effects of various kinds of high energy radiation on properties of minority carriers in silicon-doped β-Ga_2O_3. The thermal activation energy of the reference (non-irradiated) sample was 40.9 meV, which is ascribed to silicon-donors. CL measurements indicate a slightly indirect bandgap energy of 4.9 eV. Under 10 MeV proton irradiation, the thermal activation energies increase. This increase is attributable to high order defects and their influence on carrier lifetimes. Differentiating itself from other forms of radiation, neutron irradiation creates disordered regions in β-Ga_2O_3 as opposed to just point defects, resulting in the lowest carrier removal rate because of the lowest average non-ionizing energy loss.

Measurements show that β-Ga_2O_3 is more resistant to radiation damage than some other wide bandgap semiconductors due to its higher displacement threshold energy, which is inversely proportional to the lattice constant.

ACKNOWLEDGMENTS

I would like to thank my advisor Dr. Elena Flitsiyan. From the time I began at UCF, she has helped me to chart a path through the program that would lead to success. Since then she has continued to offer help and guidance both as a supervisor when I was her TA, and as a research advisor over the course of this project. Throughout my undergraduate career she has maintained her unwavering support, and I would be a lesser student and prospective scientist today without her.

I also wish to thank Dr. Richard Klemm. For most of my undergraduate career, I have worked in Dr. Klemm's research group. It was during this time that I learned what work in theoretical physics truly entails. Beyond this, Dr. Klemm has been a constant source of support and guidance in my career thus far, and I am continually grateful.

I would like to thank Dr. Robert Peale for his support of this project through his committee role. I am also thankful for his advice and support through the graduate school applications process, without which my current opportunities would not be available.

I am thankful to my family for their unconditional support both during this project, and more generally throughout my academic career.

Finally, I am thankful to God for the myriad blessings and opportunities afforded to me both professionally and personally.

TABLE OF CONTENTS

LIST OF FIGURES vi

LIST OF TABLES ix

CHAPTER 1: INTRODUCTION AND BACKGROUND 1

Semiconductors, Recombination, and Charge Carriers 1

Gallium(III) Oxide (Ga_2O_3) 3

Experimental Information 8

CHAPTER 2: RESULTS AND ANALYSIS 10

Electrical Measurements 10

Measurement and Analysis of Minority Carrier Properties 15

CL Measurements 15

CL Investigation of Neutron Irradiated Ga_2O_3 Structures 17

Effects of 10 MeV Proton Irradiation 20

CHAPTER 3: CONCLUSION 23

Bibliography 24

LIST OF FIGURES

1.1 Neutron energy spectrum from Am-Be source. The neutron energies in the Am-Be source range up to 11 MeV, with an average energy between 4 and 5 MeV. 6

1.2 Decay-diagram of ^{12}C 7

2.1 I-V Characteristic before and after two neutron doses. 11

2.2

- I-V characteristics from rectifiers before and after neutron irradiation at two different doses. (top)
- Reverse I-V characteristics from same devices (bottom). 11

2.3 Rectifier C2-V characteristics before and after neutron irradiation at varying doses 12

2.4 On/off ratio for rectifiers as a function of reverse voltage for differing neutron doses 13

2.5 Switching characteristics of rectifiers 1V forward bias to -50 V reverse bias before and after different neutron doses 13

2.6 Carrier removal rates for neutrons in this experiment compared to previous reports for different forms of radiation 14

2.7 Cathodoluminescence Apparatus. Light impacts curved mirror (b), is redirected into light guide (c), which feeds into a spectrometer/monochromator, (d). the spectrometer/monochromator output then goes to a PMT or CCD, (e) this output then is sent to a local computer (f). [1] 15

2.8 Spectral Comparison – Diode. There is a reliable observation that the intensity is higher for the sample with the larger neutron dose. . 17

2.9 Continuous wave β-Ga_2O_3 CL collected at room temperature and 6 kV accelerating voltage presented with Gaussian breakdown. The main window presents the normalized intensity spectrum (gray circles) from 300 to 600 nm with the estimated Gaussian peaks centered at 3.65 (dotted), 3.25 (dot-dashed), 2.90 eV (dashed), and the sum of the Gaussian peaks (solid). The inset presents the spectrum from 200 to 320 nm showing absence of bandgap emission [2]. 18

2.10 CL spectra for Si-doped β-Ga2O3 under accelerating voltage. The main peak was measured at approximately 380 nm, and vertical is log-scaled to ensure the visibility of the 680 nm band [1]. 19

2.11 Spectral Comparison – FET
It is observed that the intensity is higher for the sample with the larger neutron dose. The FET specimens emit a peak around 247 nm which is not seen in the diode specimens, while the band centered around 400 nm is present in both specimen types. 20

2.12 Minority carrier diffusion length in Si-doped β-Ga_2O_3 for both reference and 10 MeV proton-irradiated sample. [3] 21

LIST OF TABLES

1.1 Activation Foils 8

2.1 Parameters for Gaussian deconvolution of continuous wave CL emission of β-Ga_2O_3 [1]. 19

2.2 Properties of Si-doped β-Ga_2O_3 upon 10 MeV proton irradiation [3]. 21

CHAPTER 1: INTRODUCTION AND BACKGROUND

Semiconductors, Recombination, and Charge Carriers

Semiconductors are the foundation upon which the majority of modern technology is built. They can possess various interesting attributes including biases that allow electrical currents to flow more easily in one direction than another, variable resistances, and other useful properties.

Generally, semiconductors are characterized by their resistivity at room temperature, usually possessing the trait that their conductivity increases with temperature contrary to the behavior of most standard metals[4]. In a lattice structure, electrons can reside either in the valence energy band, or the conduction energy band where electrons move freely throughout the lattice. These bands are sometimes separated by a physically forbidden energy range referred to as a bandgap. In silicon, this bandgap is relatively narrow which allows electrons to be excited and enter the conduction band with even a small amount of heat/energy introduced into the system.

Of particular interest and relevance for all applications of semiconductors is the electrical conductivity of a given sample. The conductivity in a semiconductor depends directly on the number of free charge carriers that it contains[5]. Charge carriers are either free electrons or holes, holes being positively charged spaces left behind when free electrons move from their rest positions in the valence band. One can increase the number of carriers by introducing impurities to the lattice in a process called doping. For instance, when an

astatine atom is introduced into a pure silicon lattice, there is an extra valence electron relative to silicon that is then free to move in the lattice[6].

When an electron is in the conduction band, it can interact with a hole in the valence band in a process called recombination. Energy is released in this process since the electron that was initially in the conduction band drops to a lower energy state in the valence band after recombination. The converse process can occur as well. Given sufficient excitation, an electron can free itself from the valence band and jump into the conduction band.

If the sample is not perfectly pure (like any sample in the real world), then it will contain various impurities and defects such as excess semiconductor atoms breaking lattice symmetry, missing semiconductor atoms breaking lattice symmetry, or non-semiconductor atoms such as various metals or oxygen throughout. These imperfections can create permitted energy levels located within the semiconductor's characteristic bandgap range of energies. Shockley-Read Hall (SRH) recombination is recombination that occurs at one of these newly accessible energy levels[5].

In doped semiconductors, there is not an equal number of electrons and holes present in a given sample. For n-type semiconductors, there are more electrons than holes. In this case, holes are referred to as minority charge carriers. For p-type semiconductors, this is reversed, and the greater number of holes designates the electrons as the minority charge carriers.

Gallium(III) Oxide (Ga_2O_3)

Semiconductors with narrow bandgaps, primarily silicon, have dominated applications since the advent of the transistor. However, in recent decades there has been growing interest in semiconductors with bandgaps wider than that of the usual options. Their wider bandgap energies make them particularly interesting for high power and high temperature applications. This is due to silicon-based devices often struggling to perform as intended under such harsh conditions.

Beta gallium oxide (β-Ga_2O_3) is a particularly promising example of an ultra-wide bandgap (UWBG) semiconductor for applications in power switching electronics [7–12]. The leading motivations for the study of new UWBG semiconductors such as Ga_2O_3, BN, and high-Al AlGaN are chiefly the reduction of size, cost, and switching speeds in electronics [8, 12]. The bandgap of β-Ga_2O_3 is 4.8-4.9 eV and has an estimated critical field strength of 8 MV/cm [7, 9, 10, 12]. A bandgap of this width permits the extension of device operation into higher temperature ranges, while the magnitude of the critical field allows for operation under higher voltages [11]. The valence band is mostly flat in momentum space, which results in a very large effective mass for holes in the material, which leads to the formation of local polarons (holes confined by lattice distortions) [7, 10]. This results in one of the drawbacks of using β-Ga_2O_3 as a semiconductor, the difficulty of p-type doping of the material. Also, the thermal conductivity ($\kappa\kappa$) is approximately an order of magnitude lower than that of both SiC and GaN, and approximately half that of sapphire [12]. Finding ways to mitigate this issue such as the employment of diamond or sapphire substrates, topside active cooling, and structural variations have been of great research interest.

The resilience of wide bandgap materials is particularly advantageous in environments characterized by high temperatures and radiation dosages [3, 13–29]. In potential applications, β-Ga_2O_3-based electronics could be subjected to high energy cosmic rays, α-particles and electrons in low-Earth orbit satellites, and high energy neutron and gamma radiation in nuclear and military applications. The bonds between the gallium and oxygen atoms in β-Ga_2O_3 are extremely strong, resulting in materials based on it being quite resistant to radiation under total dose conditions [3, 20–29]. In the course of the investigation, β-Ga_2O_3 devices were irradiated with electrons, protons, alpha particles, neutrons, and gamma rays. The degradation to the devices is measured, but the degradation's functional dependence on energy and dosage remains to be confirmed. Each variety of radiation dosage inflicts differing kinds of damage on the crystal lattices [13, 14, 29]. Additionally, primary lattice defects can recombine and and form complexes with each other, dopants, and with extended defects [29].

In past investigations, most experiments studying the irradiation of β-Ga_2O_3 have been conducted using protons and α-particles since these are easier to model theoretically and perform in the lab [13]. There is comparatively little known about the effects of neutron irradiation. The effects of fast neutron irradiation on the electrical conductivity of β-Ga_2O_3 was reported by Cojocaru [30]. In that investigation, the electrical conductivity was found to decrease given a dose of 10^{17} cm^{-2}. This was explained theoretically by assuming that the lattice defects acted as electron traps. At 1000 K, the defects annealed out with an activation energy of 2 eV. β-Ga_2O_3 was irradiated with 2 MeV neutrons to a fluence of 4×10^{15} cm^{-2} by Farzana et al. [24]. This resulted in a decrease in reverse current in rectifier structures, a loss of carriers at a rate of approximately 20 cm^{-1}, and the

introduction of a deep trap state at -1.88 eV observed in deep level transient spectroscopy (DLTS) measurements. This was ascribed to an oxygen-vacancy related state. A linear increase with pulsed neutron fluence of the density of deep electron traps E2 (E_c - 1.05 eV), E3 (E_c - 1.05 eV), and E4 (E_c - 1.2 eV) admitting an introduction rate of approximately 0.5 cm^{-1} was observed.

The utility of Ga_2O_3 for detection of fast (14 MeV) neutrons using the ^{16}O (n, α)^{13}C reaction was investigated as well [27]. Under these conditions, fast neutrons could be detected, but with insufficient resolution for spectroscopy applications. Chaiken and Blue [25] reported the displacement cross-section for Ga_2O_3 subjected to neutron irradiation. The curve has a low energy cutoff since the analysis is cutoff at the neutron energy for which the maximum transferred energy is less than the threshold. The displacement damage cross-section was $\sigma(Ga_2O_{3disp})(1\ MeV) = 92.3$ MeVmb, assuming a given displacement threshold energy in Ga_2O_3 of $E_{Ga,\ d} = 25$ eV [25]. This is useful for classifying and comparing the effects of neutron irradiation under differing fluences and energies. Farzana et al. [24] characterized deep traps in bulk n-type Sn-doped Ga_2O_3 subjected to neutron irradiation up to fluences of 2×10^{15} cm^{-2}. An increase in concentration of electron traps E3 (E_c - 1.05 eV) and E1 (E_c - 0.65 eV) in DLTS and an increase in the occurrence of hole traps with an optical threshold approaching 2 eV was observed, which is in general agreement with the results that have been reported for proton-irradiated crystals [3, 24].

In this project, we report on the effects α-particle radiation on the material properties of Ga_2O_3 rectifiers. The neutron sources consist of an alpha emitter (Am-241 in our case) mixed with a low Z material, usually ^9Be. Neutrons are emitted in the reaction:

$$^{9}\mathrm{Be}+\alpha \longrightarrow {}^{12}\mathrm{C}+\mathrm{neutron}+\gamma\,(4.44\ \mathrm{MeV}).$$

The energies commonly range up to 11 MeV, with an average energy of 4.2 MeV as shown in Figure 1.1. In Ga_2O_3, the mean free path is over 10 cm, much larger than the thickness of the given samples [28]. The narrow scattering cross-section of $\leq$0.5 cm^{-1} suggests the average number of interactions per neutron is on the order of 10^6 reactions/cm^{-2} for the drift region of the rectifier structure at the highest dosage condition.

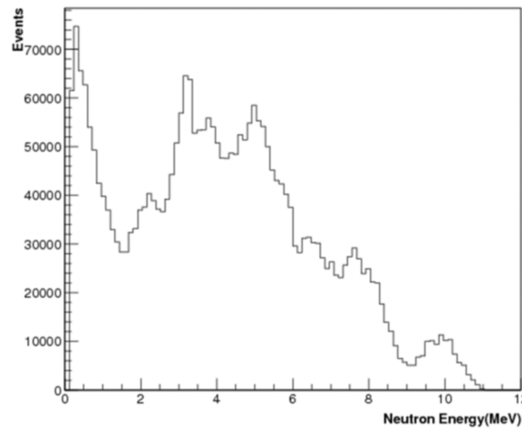

Figure 1.1: Neutron energy spectrum from Am-Be source. The neutron energies in the Am-Be source range up to 11 MeV, with an average energy between 4 and 5 MeV.

α-particles are emitted via radioactive decay of ^{241}Am [31]. The half-life of the ^{241}Am α-emitter is around 400 years, so the intensity is generally unchanged over the course of the experiment. The resultant ^{12}C nucleus emits 4.44 MeV gamma-rays along with the neutrons. Consequently, the ^{241}Am-Be source can also be used as a mono-energetic high

energy gamma-ray source.

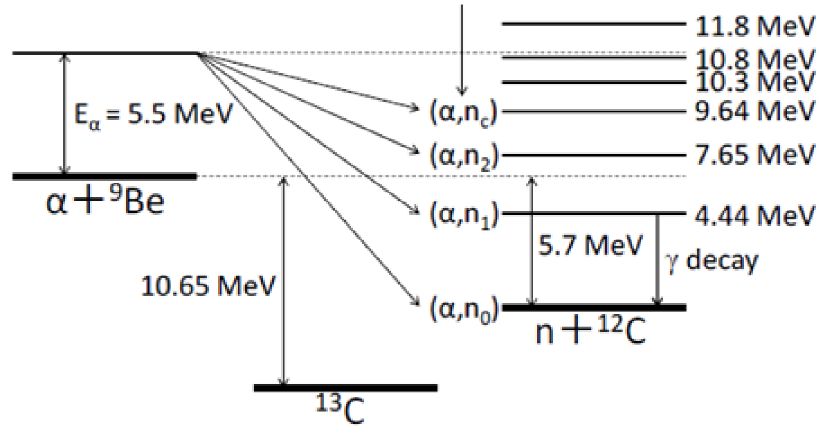

Figure 1.2: Decay-diagram of ^{12}C

It is found that the reverse current and on/off ratio in the Ga_2O_3 rectifiers are sensitive to neutron doses around 5×10^{12} cm^{-2}, characterized by carrier removal rates of approximately 0.480 cm^{-1}. The reverse recovery time ($\sim$27 ns) and the diode ideality factor were unaffected by doses in this range.

In order to estimate the exact neutron dosage in the sample, reference activation foils with well-known cross-sections in the given energy ranges were used. The threshold cross-sections and reaction types of the activated elements are shown in table 1.1 on the following page.

Nucleus	Nuclear Reaction	Reaction Threshold (MeV)
^{115}In	(n, n')	0.8
^{111}Cd	(n, n')	0.9
^{64}Zn	(n, p)	2.5
^{27}Al	(n, p)	4.2
^{27}Al	(n, α)	7.0

Table 1.1: Activation Foils

Experimental Information

The fabrication sequence for the Schottky rectifiers began with a layer structure of 10 μm Si-doped (3.5 $\times$ 10^{16} cm^{-3}) epitaxial layer grown by Halide Vapor Epitaxy (HVPE) on an (001) oriented 650 μm β-phase Sn-doped (n = 3.6 $\times$ 10^{18} cm^{-3}) Ga_2O_3 substrate (Novel Crystal Technology). A full area backside Ohmic contact (20 nm / 80 nm, Ti / Au) was deposited by electron beam evaporation and annealed for 30 s at 550° C in N_2 in a rapid thermal annealer. To form a field plate, 40 nm Al_2O_3 and 360 nm SiNx dielectric were deposited using Atomic Layer Deposition and Plasma Enhanced Chemical Vapor Deposition respectively. Windows with 100 μm diameter were opened using 1:10 diluted Buffered Oxide Etchant (BOE). The sample surface was then treated in O_3 for 20 minutes to remove contamination species including hydrocarbons. 400 μm Ni/Au (80 nm/320 nm) Schottky metal was subsequently deposited using electron beam evaporation with standard acetone lift-off.

The samples were exposed to the neutron source at cumulative doses of 10^{12} or 5 $\times$ 10^{12} cm^{-2}. They were then characterized for changes in various parameters including current-

voltage (I-V), capacitance-voltage (C-V), reverse recovery, on/off ratio, Schottky barrier height and diode ideality factor with the forward I-V characteristics, Cathodoluminescent (CL) spectrum, and EBIC (Electron Beam Induced Current) techniques.

CHAPTER 2: RESULTS AND ANALYSIS

Electrical Measurements

In Figure 2.1, we have the I-V characteristic before and after two doses of neutron radiation. The forward portion of the characteristic exhibits no measurable change after irradiation, with the Schottky barrier height maintaining it's initial value of 0.76 ± 0.05 eV, and the diode ideality factor invariant at 1.15 ± 0.03. The on-state resistance also remained at its reference value of 3.5 ± 0.1 mΩcm^2. However, the reverse current was found to increase for both doses, as seen in the bottom of Figure 2.1. This indicates the formation of recombination centers that increased the reverse current, which itself is fixed by the sum of the saturation and generation currents in the sample. The primary displacement defects introduced in the irradiation of Ga_2O_3 are expected to be oxygen and gallium vacancies [27–30, 32]. The former are deep donors, and thus do not induce n-type conductivity at standard temperatures in Ga_2O_3. The gallium vacancies are triple acceptors, which can compensate for the background n-type conductivity in Ga_2O_3. Kananen et al. [32] irradiated a sample with high energy neutrons, which created vacancies and lowered the Fermi energy below the (2-/3-) level. This results in the V_{Ga}^{2-} defect, which has one unpaired spin-$\frac{1}{2}$ located on one of the O(I) atoms near the vacancy [8]. Positron annihilation experiments have confirmed that V_{Ga} is a compensating acceptor in n-type Ga_2O_3 [8].

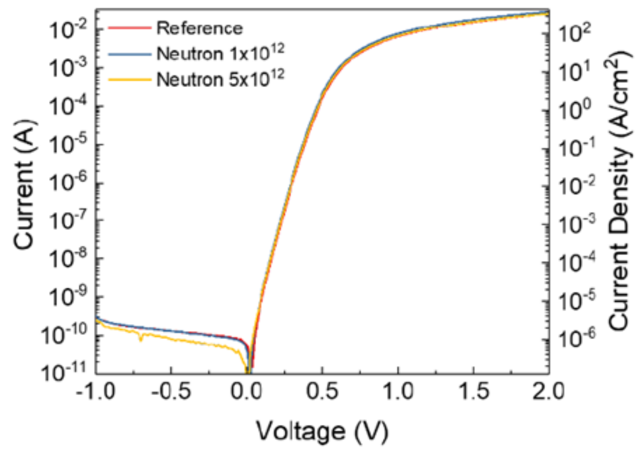

Figure 2.1: I-V Characteristic before and after two neutron doses.

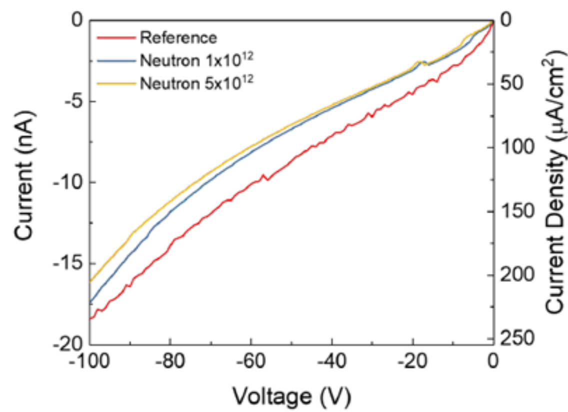

Figure 2.2:
- I-V characteristics from rectifiers before and after neutron irradiation at two different doses. (top)
- Reverse I-V characteristics from same devices (bottom).

In Figure 2.2, it is shown in the C2-V characteristics that carrier concentration in the drift region of the rectifiers was decreased upon irradiation. From the slope of these plots, we

extract carrier concentrations of 1.36×10^{16} cm^{-3} in the reference device, and 1.18×10^{16} cm^{-3} and 1.12×10^{12} cm^{-3} respectively for the doses of 10^{12} and 5×10^{12} cm^{2}. The effective carrier removal rate throughout was 480 cm^{-1}. The compensation of the n-type doping indicates that acceptors were created upon neutron irradiation, consistent with the observation regarding V_{Ga} earlier on.

In Figure 2.4, the rectifier on/off ratio is measured at 1V forward, and then reverse biases in the range of 0-100 V are shown. A clear decrease in this parameter is observed for the higher neutron dosage due to the more extreme increase in reverse current.

This is in sharp contrast with Figure 2.5. Here, the reverse recovery time when switching from +1 V forward to -10 V reverse bias voltage is invariant with respect to neutron flux over the investigated range and remains at 27 ns for all rectifiers.

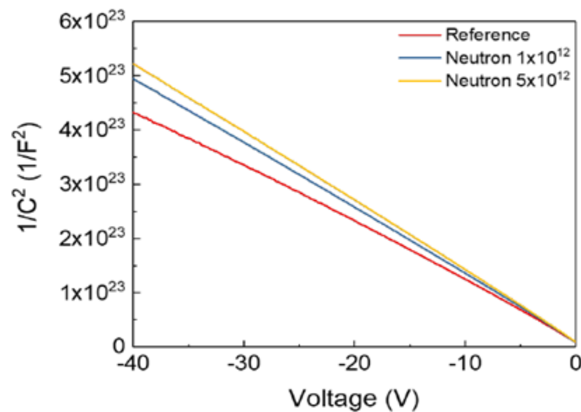

Figure 2.3: Rectifier C2-V characteristics before and after neutron irradiation at varying doses

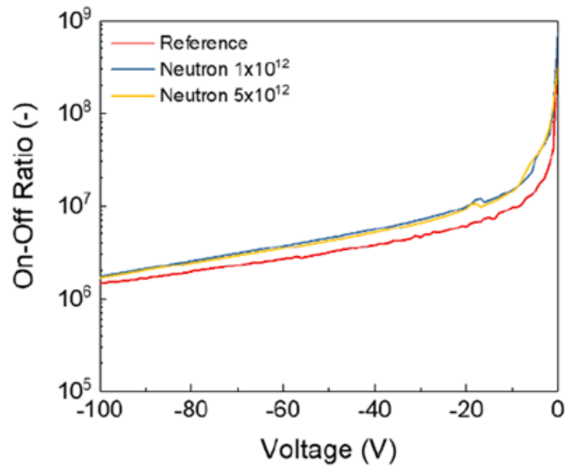

Figure 2.4: On/off ratio for rectifiers as a function of reverse voltage for differing neutron doses

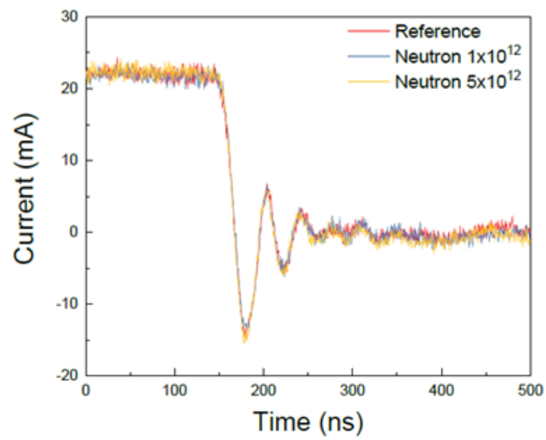

Figure 2.5: Switching characteristics of rectifiers 1V forward bias to -50 V reverse bias before and after different neutron doses

Another topic of interest is the comparison between the results of neutron irradiation from the Am-Be source, with other reports in the literature using varying neutron energies and other kinds of radiation [29]. Below, Figure 2.6 displays a compilation of this data. It should be noted that there is some inherent uncertainty in the reported values. This is due to the fact that it is not always clear that the removal rates were measured under conditions with linear dosage and moreover, high levels of compensating impurities or of extended defects created during the irradiation process can also affect the effective removal rate[15–17, 19]. However, it is clear that gamma and electron radiation are the least damaging to Ga_2O_3 while alpha particles are the most damaging. The reported value for neutrons with an average energy of 4.2 MeV is roughly 20 times higher than for neutrons with an average energy of 1 MeV.

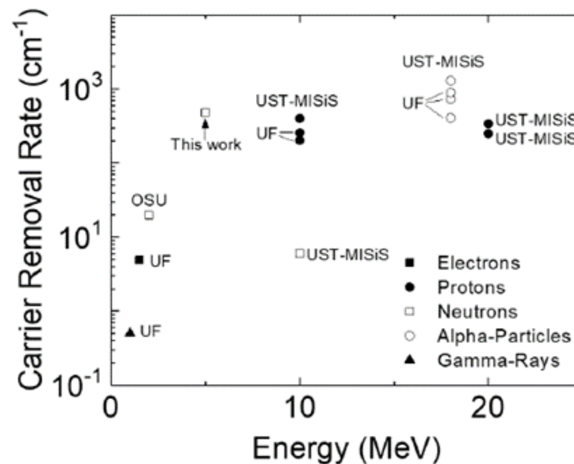

Figure 2.6: Carrier removal rates for neutrons in this experiment compared to previous reports for different forms of radiation

CL Measurements

In this section, we study the effects of high energy radiation on minority carrier diffusion lengths in silicon-doped β-Ga_2O_3. The thermal activation energy found in the non-irradiated samples was 40.9 meV. Cathodoluminescence measurements indicate a slightly indirect bandgap energy of 4.9 eV. Under electron radiation of 1.5 MeV, activation energies are found to decrease. Alternatively, they increase under 10 MeV proton irradiation. The higher activation energy under proton irradiation is ascribable to high order lattice defects that affect carrier lifetimes. In-situ CL measurements were performed with a SEM.

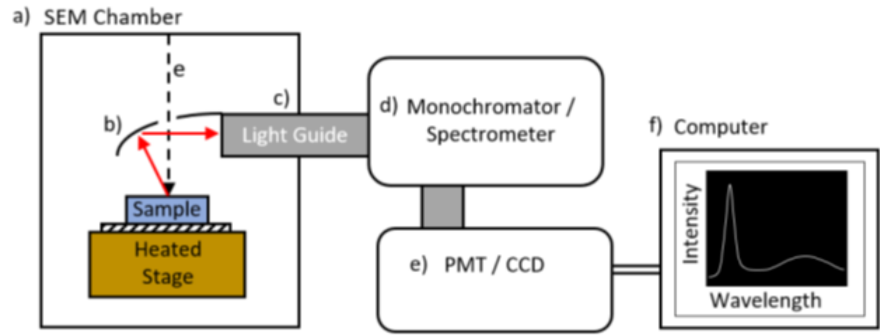

Figure 2.7: Cathodoluminescence Apparatus. Light impacts curved mirror (b), is redirected into light guide (c), which feeds into a spectrometer/monochromator, (d). the spectrometer/monochromator output then goes to a PMT or CCD, (e) this output then is sent to a local computer (f). [1]

Charge traps have an activation energy that is obtained through recording intensity, as there exists a convenient relation between the CL intensity (I_{CL}) and temperature:

$$I_{CL}(T) = \frac{A}{1 + B\exp(-\frac{E_\alpha}{k_B T})} \tag{2.1}$$

where E_α is the carrier activation energy and A and B are scaling constants. A constant temperature is maintained for at least five minutes before any data is collected during the measurement process. At equilibrium, there is a direct proportional relation between CL intensity and temperature, and an inverse proportional relation between the CL intensity and the minority carrier lifetime.

Interactions with the electron beam can cause traps to become occupied over time and affect the observed intensity. This leads to a time dependence of the CL intensity. Given that I_{CL} is inversely proportional to minority carrier lifetime, it can be found that:

$$I_{CL}^{-1} \propto \tau = \frac{L_0^2}{D}\exp\left(-\frac{E_\alpha}{k_B T}\right) \tag{2.2}$$

which also implies that L_0 has a nontrivial time dependence under continual excitation from the electron beam [33]. The rate that L_0 grows can then be found by recording the intensity as the temperature varies. One can then find a rate given by:

$$R(T) = R_0\exp\left(-\frac{E_\alpha}{k_B T}\right) \tag{2.3}$$

where R_0 is an arbitrary constant.

There have also been investigations of various optical properties given varying dopants. Dopant atoms with a charge magnitude greater than three resulted in an emission around 380 to 400 nm, and both beryllium and lithium result in emission around 500 nm [34].

Emission properties of β-Ga_2O_3 have also been studied to determine dopant species and concentrations [34, 35]. Dopant atoms with a charge magnitude greater than three resulted in an emission near 380-400 nm and doping with either beryllium or lithium result in emission around 500 nm [34].

CL Investigation of Neutron Irradiated Ga_2O_3 Structures

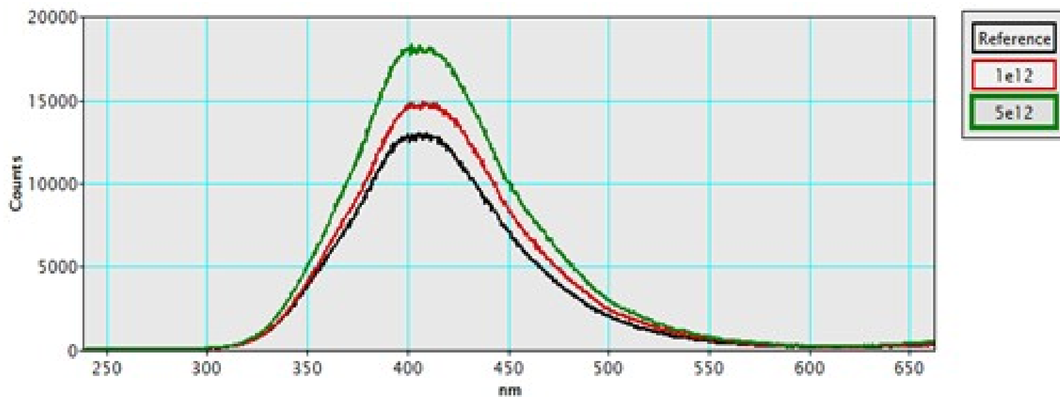

Figure 2.8: Spectral Comparison – Diode. There is a reliable observation that the intensity is higher for the sample with the larger neutron dose.

Gallium oxide's bandgap is usually assumed to be direct and is around 4.9 eV, and measurements place the cutoff wavelength at approximately 259 nm [34, 36]. However, β-Ga_2O_3's bandgap is slightly indirect and there is no emission at the bandgap energy. The

other bands with observable emissions lie below the bandgap energy and are approximated as Gaussian energy bands. The 3.65 eV band is attributable to charge transitions one of the oxygen vacancies [37], the 3.25 eV band is associated to free electrons recombining with self-trapped holes [38], and the band at 2.9 eV is associated to donor-acceptor pairs [36].

The dominant peak was measured at approximately 380 nm, and the the CL emission data with a Gaussian fit is presented below:

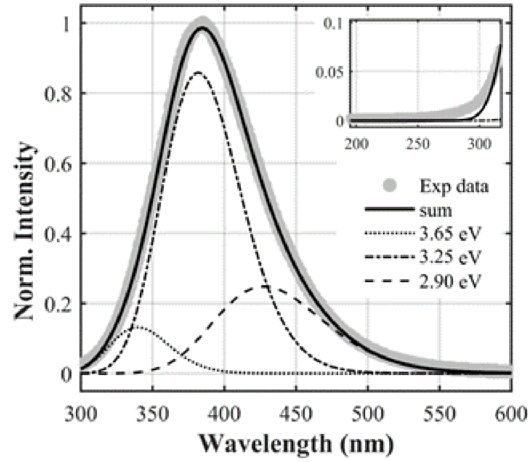

Figure 2.9: Continuous wave β-Ga_2O_3 CL collected at room temperature and 6 kV accelerating voltage presented with Gaussian breakdown. The main window presents the normalized intensity spectrum (gray circles) from 300 to 600 nm with the estimated Gaussian peaks centered at 3.65 (dotted), 3.25 (dot-dashed), 2.90 eV (dashed), and the sum of the Gaussian peaks (solid). The inset presents the spectrum from 200 to 320 nm showing absence of bandgap emission [2].

In figure 2.9, it can be seen that there is no emission at 4.9 eV, which is consistent with previous studies. The CL intensity was shown to change with accelerating voltage, and this is shown below in Figure 2.10.

Band Energy	a_i (a.u.)	b_i (eV)	c_i (eV)	$FWHM_i$ (eV)
E_1 = 3.65 eV	0.13	3.65	0.31	0.52
E_2 = 3.25 eV	0.86	3.25	0.33	0.55
E_3 = 2.90 eV	0.25	2.90	0.36	0.60

Table 2.1: Parameters for Gaussian deconvolution of continuous wave CL emission of β-Ga_2O_3 [1].

Also presented are emission spectra out to further wavelength values, exhibiting a band at approximately 680 nm due to defects. The current value of the beam for the 6 and 8 kV values are nearly the same, while their associated emission values are not. Consequently, it is concluded that the dependence of CL intensity on accelerating voltage is significant. This can be explained by noting that the generation volume of the system may enclose carriers that are capable of radiative recombination.

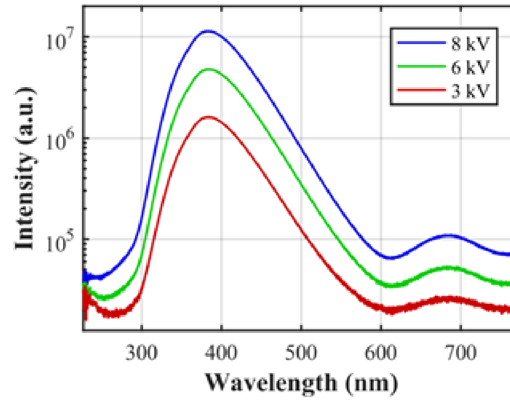

Figure 2.10: CL spectra for Si-doped β-Ga2O3 under accelerating voltage. The main peak was measured at approximately 380 nm, and vertical is log-scaled to ensure the visibility of the 680 nm band [1].

A spectral comparison of intensities observed in FET's under varying neutron dosages is

also given below.

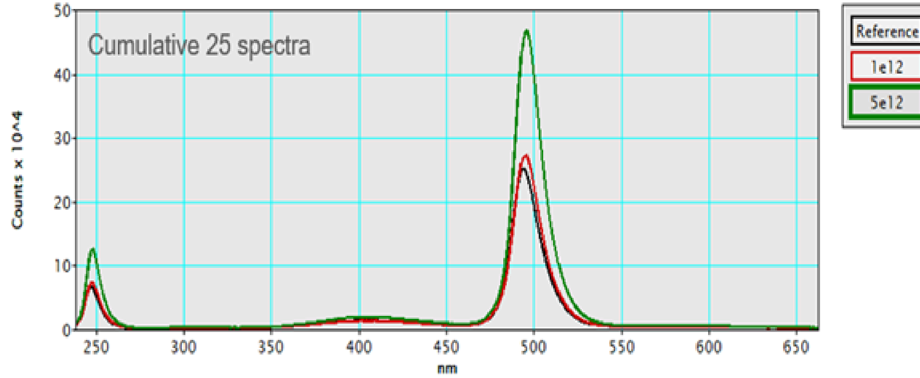

Figure 2.11: Spectral Comparison – FET
It is observed that the intensity is higher for the sample with the larger neutron dose. The FET specimens emit a peak around 247 nm which is not seen in the diode specimens, while the band centered around 400 nm is present in both specimen types.

Effects of 10 MeV Proton Irradiation

The rates of carrier removal in β-Ga_2O_3 dosed with proton radiation are found to be close to those of GaN with similar doping under comparable dosage conditions [39, 40]. The most common defect to arise in Ga_2O_3 under these conditions is a gallium vacancy with two hydrogens [41].

The electron beam induced current method was used to find the minority carrier diffusion length (L) before and after dosage. At room temperature, L was approximately 340nm in the reference sample. This value decreased with increases in temperature. After the dosage with proton radiation, the value of L at room temperature decreased to approxi-

mately 315 nm. For the reference sample, the activation energy was 41.8 meV and L_0 was approximately 145 nm. For the irradiated sample, these values approached 16.2 meV and 228 nm respectively.

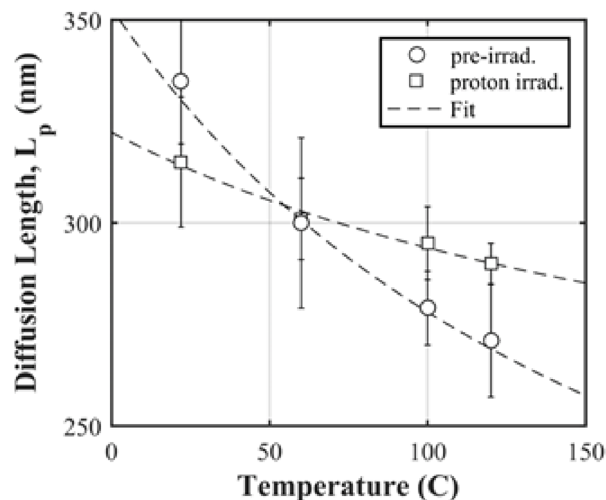

Figure 2.12: Minority carrier diffusion length in Si-doped β-Ga_2O_3 for both reference and 10 MeV proton-irradiated sample. [3]

The diffusion length's dependence on temperature implies that the defects tend to protect it against reduction due to temperature at temperatures greater than 60 °C.

Fluence	n (cm^{-3})	L (nm)	L_0 (nm)	E_a (meV)	τ (ps)
0 (Reference Sample)	3.1×10^{16}	340 ± 22	145	41.8	215 ± 22
1×10^{14}	8.03×10^{15}	315 ± 16	228	16.2	300 ± 35

Table 2.2: Properties of Si-doped β-Ga_2O_3 upon 10 MeV proton irradiation [3].

Removal of carriers in the epilayer through non-ionizing energy loss was observed. This resulted in the creation of both electron traps, and hole acceptors, which served to com-

pensate for the doping. The rate of carrier removal was calculated to be 235.7 cm^{-1} under dosage. Also, carrier density dropped from an initial 3.1×10^{16} cm^{-3} to 8.03×10^{15} cm^{-3} after dosage. This was restored to 1.87×10^{16} cm^{-3} after annealing at 300 °C.

CHAPTER 3: CONCLUSION

There is an observed decrease in the diffusion length of minority carriers with decreases in temperature in all β-Ga_2O_3 samples. This is not what happens in GaN [18] but is consistent with results for Si and GaP [25]. When the samples are subjected to high energy electron and proton irradiation, the diffusion lengths of minority carriers decreases. The activation energies are close to the ionization energy of donors in previous β-Ga_2O_3 studies [42–46].

LIST OF REFERENCES

[1] Jonathan Lee. Impact of Ionizing Radiation and Electron Injection on Carrier Transport Properties in Narrow and Wide Bandgap Semiconductors. *Electronic Theses and Dissertations*, January 2018.

[2] Jonathan Lee, Elena Flitsiyan, Leonid Chernyak, Jiancheng Yang, Fan Ren, Stephen J. Pearton, Boris Meyler, and Y. Joseph Salzman. Effect of 1.5 MeV electron irradiation on β-Ga_2O_3 carrier lifetime and diffusion length. *Appl. Phys. Lett.*, 112(8):082104, February 2018. Publisher: American Institute of Physics.

[3] Jiancheng Yang, Zhiting Chen, Fan Ren, S. J. Pearton, Gwangseok Yang, Jihyun Kim, Jonathan Lee, Elena Flitsiyan, Leonid Chernyak, and Akito Kuramata. 10 MeV proton damage in β-Ga_2O_3 Schottky rectifiers. *Journal of Vacuum Science & Technology B*, 36(1):011206, January 2018. Publisher: American Vacuum Society.

[4] Charles Kittel. *Introduction to Solid State Physics*. Wiley, Hoboken, NJ, 8th edition edition, November 2004.

[5] J.-P. Colinge and C. A. Colinge. *Physics of Semiconductor Devices*. Kluwer Academic Publishers, Boston, 2002nd edition edition, May 2002.

[6] Chenming C. Hu. *Modern Semiconductor Devices for Integrated Circuits*. PEARSON INDIA, 1st edition edition, January 2009.

[7] Zbigniew Galazka. β-Ga_2O_3 for wide-bandgap electronics and optoelectronics. *Semicond. Sci. Technol.*, 33(11):113001, November 2018.

[8] S. J. Pearton, Jiancheng Yang, Patrick H. Cary, F. Ren, Jihyun Kim, Marko J. Tadjer, and Michael A. Mastro. A review of Ga_2O_3 materials, processing, and devices. *Applied Physics Reviews*, 5(1):011301, March 2018.

[9] Hongpeng Zhang, Lei Yuan, Xiaoyan Tang, Jichao Hu, Jianwu Sun, Yimen Zhang, Yuming Zhang, and Renxu Jia. Progress of Ultra-Wide Bandgap Ga_2O_3 Semiconductor Materials in Power MOSFETs. *IEEE Transactions on Power Electronics*, 35(5):5157–5179, May 2020. Conference Name: IEEE Transactions on Power Electronics.

[10] Elaheh Ahmadi and Yuichi Oshima. Materials issues and devices of α and β-Ga_2O_3. *Journal of Applied Physics*, 126(16):160901, October 2019. Publisher: American Institute of Physics.

[11] S. J. Pearton, Fan Ren, Marko Tadjer, and Jihyun Kim. Perspective: Ga_2O_3 for ultra-high power rectifiers and MOSFETS. *Journal of Applied Physics*, 124(22):220901, December 2018. Publisher: American Institute of Physics.

[12] Jingjing Xu, Wei Zheng, and Feng Huang. Gallium oxide solar-blind ultraviolet photodetectors: a review. *J. Mater. Chem. C*, 7(29):8753–8770, July 2019. Publisher: The Royal Society of Chemistry.

[13] J. R. Srour and J. W. Palko. Displacement Damage Effects in Irradiated Semiconductor Devices. *IEEE Transactions on Nuclear Science*, 60(3):1740–1766, June 2013. Conference Name: IEEE Transactions on Nuclear Science.

[14] J. Nord, K. Nordlund, and J. Keinonen. Molecular dynamics study of damage ac-

cumulation in GaN during ion beam irradiation. *Physical Review B*, 68:184104, November 2003. ADS Bibcode: 2003PhRvB..68r4104N.

[15] S. J. Pearton, Ya-Shi Hwang, and F. Ren. Radiation Effects in GaN-Based High Electron Mobility Transistors. *JOM*, 67(7):1601–1611, July 2015.

[16] Alexander Y. Polyakov, S. J. Pearton, Patrick Frenzer, Fan Ren, Lu Liu, and Jihyun Kim. Radiation effects in GaN materials and devices. *J. Mater. Chem. C*, 1(5):877–887, January 2013. Publisher: The Royal Society of Chemistry.

[17] Stephen J. Pearton, Richard Deist, Fan Ren, Lu Liu, Alexander Y. Polyakov, and Jihyun Kim. Review of radiation damage in GaN-based materials and devices. *Journal of Vacuum Science & Technology A*, 31(5):050801, September 2013. Publisher: American Vacuum Society.

[18] Cameron L. Tracy, Maik Lang, Daniel Severin, Markus Bender, Christina Trautmann, and Rodney C. Ewing. Anisotropic expansion and amorphization of Ga_2O_3 irradiated with 946MeV Au ions. *Nuclear Instruments and Methods in Physics Research Section B: Beam Interactions with Materials and Atoms*, 374:40–44, May 2016.

[19] S. J. Pearton, F. Ren, Erin Patrick, M. E. Law, and Alexander Y. Polyakov. Review—Ionizing Radiation Damage Effects on GaN Devices. *ECS J. Solid State Sci. Technol.*, 5(2):Q35, November 2015. Publisher: IOP Publishing.

[20] Jiancheng Yang, Fan Ren, Stephen J. Pearton, Gwangseok Yang, Jihyun Kim, and Akito Kuramata. 1.5MeV electron irradiation damage in β-Ga_2O_3 vertical rectifiers.

Journal of Vacuum Science & Technology B, 35(3):031208, May 2017. Publisher: American Vacuum Society.

[21] Jiancheng Yang, Chaker Fares, Yu Guan, F. Ren, S. J. Pearton, Jinho Bae, Jihyun Kim, and Akito Kuramata. Eighteen mega-electron-volt alpha-particle damage in homoepitaxial β-Ga_2O_3 Schottky rectifiers. *Journal of Vacuum Science & Technology B*, 36(3):031205, May 2018. Publisher: American Vacuum Society.

[22] Man Hoi Wong, Akinori Takeyama, Takahiro Makino, Takeshi Ohshima, Kohei Sasaki, Akito Kuramata, Shigenobu Yamakoshi, and Masataka Higashiwaki. Radiation hardness of Ga_2O_3 MOSFETs against gamma-ray irradiation. In *2017 75th Annual Device Research Conference (DRC)*, pages 1–2, June 2017.

[23] Jihyun Kim, Stephen J. Pearton, Chaker Fares, Jiancheng Yang, Fan Ren, Suhyun Kim, and Alexander Y. Polyakov. Radiation damage effects in Ga_2O_3 materials and devices. *J. Mater. Chem. C*, 7(1):10–24, December 2018. Publisher: The Royal Society of Chemistry.

[24] Esmat Farzana, Akhil Mauze, Joel B. Varley, Thomas E. Blue, James S. Speck, Aaron R. Arehart, and Steven A. Ringel. Influence of neutron irradiation on deep levels in Ge-doped (010) β-Ga_2O_3 layers grown by plasma-assisted molecular beam epitaxy. *APL Materials*, 7(12):121102, December 2019. Publisher: American Institute of Physics.

[25] Max F. Chaiken and Thomas E. Blue. An Estimation of the Neutron Displacement Damage Cross Section for Ga2O3. *IEEE Transactions on Nuclear Science*,

65(5):1147–1152, May 2018. Conference Name: IEEE Transactions on Nuclear Science.

[26] A. Y. Polyakov, N. B. Smirnov, I. V. Shchemerov, A. A. Vasilev, E. B. Yakimov, A. V. Chernykh, A. I. Kochkova, P. B. Lagov, Yu S. Pavlov, O. F. Kukharchuk, A. A. Suvorov, N. S. Garanin, In-Hwan Lee, Minghan Xian, Fan Ren, and S. J. Pearton. Pulsed fast reactor neutron irradiation effects in Si doped n-type β-Ga_2O_3. *J. Phys. D: Appl. Phys.*, 53(27):274001, May 2020. Publisher: IOP Publishing.

[27] D. Szalkai, Z. Galazka, K. Irmscher, P. Tüttő, A. Klix, and D. Gehre. β-Ga_2O_3 Solid-State Devices for Fast Neutron Detection. *IEEE Transactions on Nuclear Science*, 64(6):1574–1579, June 2017. Conference Name: IEEE Transactions on Nuclear Science.

[28] Patrick H. Carey, Fan Ren, Michael A. Sedlack, Elena Flitsiyan, and Stephen J. Pearton. Neutron Irradiation of AlGaN Polarization Doped Field Effect Transistors. *ECS J. Solid State Sci. Technol.*, 9(6):065007, July 2020. Publisher: The Electrochemical Society.

[29] S. J. Pearton, Assel Aitkaliyeva, Minghan Xian, Fan Ren, Ani Khachatrian, Adrian Ildefonso, Zahabul Islam, Md Abu Jafar Rasel, Aman Haque, A. Y. Polyakov, and Jihyun Kim. Review—Radiation Damage in Wide and Ultra-Wide Bandgap Semiconductors. *ECS J. Solid State Sci. Technol.*, 10(5):055008, May 2021. Publisher: The Electrochemical Society.

[30] L. N. Cojocaru. Defect-annealing in neutron-damaged β-Ga_2O_3. *Radiation*

Effects, 21(3):157–160, January 1974. Publisher: Taylor & Francis _eprint: https://doi.org/10.1080/00337577408241456.

[31] O. Aktas, A. Kuliev, V. Kumar, R. Schwindt, S. Toshkov, D. Costescu, J. Stubbins, and I. Adesida. 60Co gamma radiation effects on DC, RF, and pulsed I-V characteristics of AlGaN/GaN HEMTs. *Solid-State Electronics*, 48(3):471–475, March 2004.

[32] B. E. Kananen, L. E. Halliburton, K. T. Stevens, G. K. Foundos, and N. C. Giles. Gallium vacancies in β-Ga_2O_3 crystals. *Appl. Phys. Lett.*, 110(20):202104, May 2017. Publisher: American Institute of Physics.

[33] W. C. Burdett, O. Lopatiuk, A. Osinsky, S. J. Pearton, and L. Chernyak. The optical signature of electron injection in p-(Al)GaN. *Superlattices and Microstructures*, 34(1):55–62, July 2003.

[34] G. Blasse and A. Bril. Some observations on the luminescence of β-Ga_2O_3. *Journal of Physics and Chemistry of Solids*, 31(4):707–711, April 1970.

[35] T. Harwig and F. Kellendonk. Some observations on the photoluminescence of doped -galliumsesquioxide. *Journal of Solid State Chemistry*, 24(3):255–263, April 1978.

[36] Kiyoshi Shimamura, Encarnación G. Víllora, Takekazu Ujiie, and Kazuo Aoki. Excitation and photoluminescence of pure and Si-doped β-Ga_2O_3 single crystals. *Appl. Phys. Lett.*, 92(20):201914, May 2008. Publisher: American Institute of Physics.

[37] Joel Varley, Justin Weber, Anderson Janotti, and C. Walle. Oxygen vacancies and donor impurities in β-Ga_2O_3. *Applied Physics Letters*, 97, October 2010.

[38] J. B. Varley, A. Janotti, C. Franchini, and C. G. Van de Walle. Role of self-trapping in luminescence and p-type conductivity of wide-bandgap oxides. *Phys. Rev. B*, 85(8):081109, February 2012. Publisher: American Physical Society.

[39] Shihyun Ahn, Yi-Hsuan Lin, Fan Ren, Sooyeoun Oh, Younghun Jung, Gwangseok Yang, Jihyun Kim, Michael A. Mastro, Jennifer K. Hite, Charles R. Eddy, and Stephen J. Pearton. Effect of 5 MeV proton irradiation damage on performance of β-Ga_2O_3 photodetectors. *Journal of Vacuum Science & Technology B*, 34(4):041213, July 2016. Publisher: American Vacuum Society.

[40] Jiancheng Yang, Shihyun Ahn, F. Ren, S. J. Pearton, Soohwan Jang, Jihyun Kim, and A. Kuramata. High reverse breakdown voltage Schottky rectifiers without edge termination on Ga_2O_3. *Appl. Phys. Lett.*, 110(19):192101, May 2017. Publisher: American Institute of Physics.

[41] Philip Weiser, Michael Stavola, W. Beall Fowler, Ying Qin, and Stephen Pearton. Structure and vibrational properties of the dominant O-H center in β-Ga_2O_3. *Appl. Phys. Lett.*, 112(23):232104, June 2018. Publisher: American Institute of Physics.

[42] Laurent Binet and Didier Gourier. ORIGIN OF THE BLUE LUMINESCENCE OF β-Ga_2O_3. *Journal of Physics and Chemistry of Solids*, 59(8):1241–1249, August 1998.

[43] Toshiyuki Oishi, Yuta Koga, Kazuya Harada, and Makoto Kasu. High-mobility β-Ga_2O_3 single crystals grown by edge-defined film-fed growth method and their Schottky barrier diodes with Ni contact. *Appl. Phys. Express*, 8(3):031101, February 2015. Publisher: IOP Publishing.

[44] K. Irmscher, Z. Galazka, M. Pietsch, R. Uecker, and R. Fornari. Electrical properties of β-Ga_2O_3 single crystals grown by the Czochralski method. *Journal of Applied Physics*, 110(6):063720, September 2011. Publisher: American Institute of Physics.

[45] Jonathan R. I. Lee, E. Flitsiyan, L. Chernyak, Shihyun Ahn, F. Ren, Lin Yuna, S. Pearton, J. Kim, B. Meyler, and J. Salzman. Optical Signature of the Electron Injection in Ga_2O_3. 2017.

[46] N. T. Son, K. Goto, K. Nomura, Q. T. Thieu, R. Togashi, H. Murakami, Y. Kumagai, A. Kuramata, M. Higashiwaki, A. Koukitu, S. Yamakoshi, B. Monemar, and E. Janzén. Electronic properties of the residual donor in unintentionally doped β-Ga_2O_3. *Journal of Applied Physics*, 120(23):235703, December 2016. Publisher: American Institute of Physics.